

# The Effects of Cr and Mo on the Microstructure and Mechanical Properties of As-Cast TiAl Alloys

Husni<sup>1</sup>, Ahmad Fauzi Mohd. Noor<sup>2</sup> & Rizal Astrawinata<sup>2</sup>

<sup>1</sup>Program Studi Teknik Pertambangan, Fakultas Teknik, Universitas Syiah Kuala, Jl. Tgk. Syech A. Rauf No. 7, Darussalam, Banda Aceh 23111, Indonesia
<sup>2</sup>School of Materials and Mineral Resources Engineering, Universiti Sains Malaysia, Engineering Campus, 14300 Nibong Tebal, Pulau Penang, Malaysia
E-mail: husni.usman@gmail.com

Abstract. The effect of the alloying elements of Cr and Mo on the microstructure and mechanical properties of as-cast TiAl alloys produced by a locally made arc-melting furnace was studied. X-ray diffraction (XRD) was used to identify the phases present in the samples. The microstructure of the TiAl samples was characterized using scanning electron microscopy combined with energy dispersive spectroscopy (EDS). Compression tests were carried out at room temperature using an Instron servohydraulic testing machine. The results show that the Ti-48Al alloy exhibited a duplex microstructure, whereas with the addition of Cr a nearly lamellar microstructure was observed in Ti-48Al-2Cr and with the addition of both Cr and Mo also in Ti-48Al-2Cr-2Mo. The hardness values increased slightly as compared to the Ti-48Al alloy with the addition of the alloying elements. The presence of Cr in Ti-48Al-2Cr resulted in a slight increase in compressive fracture strain. The as-cast Ti-48Al-2Cr-2Mo alloy produced a higher yield strength and fracture strain in compression as compared to the other as-cast TiAl alloys. On the fracture surfaces of the as-cast TiAl alloys, mixed brittle transgranular and interlamellar fracture modes were predominantly observed.

**Keywords:** alloying elements; as-cast TiAl alloys; fracture behavior; mechanical properties; microstructure.

#### 1 Introduction

Currently, there is an increase in demand for the development of energy conversion systems with improved efficiency and ecological compatibility. Higher operating temperatures, lighter weight and higher operation speeds are required for advanced design concepts. Presently, the limits of material capability of conventional metallic systems such as titanium alloy IMI834 are reported to have reached their maximum height [1,2]. New classes of materials will be required if further advancement is to be made. Intermetallic  $\gamma$ -TiAlbased alloys are widely recognized as having the potential to meet the design requirements mentioned above because of their low possible density (3.9-4.1

Received January 18<sup>th</sup>, 2012, 1<sup>st</sup> Revision May 29<sup>th</sup>, 2013, 2<sup>nd</sup> Revision September 16<sup>th</sup>, 2013, Accepted for publication October 1<sup>st</sup>, 2013

Copyright © 2013 Published by ITB Journal Publisher, ISSN: 2337-5779, DOI: 10.5614/j.eng.technol.sci.2013.45.3.6

gr/cm $^3$ ), high specific yield strength, high specific stiffness, low diffusion coefficient, good structural stability, good creep resistance, and excellent oxidation resistance at high temperatures [3-5]. Based on these attractive properties,  $\gamma$ -TiAl-based alloys can be considered for use in a wide range of components in the automotive industry, power plant turbines and aircraft turbine engines. Ultimately, the expectation is the heavier nickel or iron-based superalloys in these applications to be substituted.

The constituent phases of  $\gamma$ -TiAl alloys always consist of  $\gamma$ -TiAl (ordered face-centered tetragonal L10 structure) as the matrix phase and  $\alpha_2$ -Ti3Al (ordered hexagonal DO19 structure) as the major second phase [4,6]. TiAl alloys without  $\alpha_2$ -Ti3Al phase, even with low interstitial impurity levels (< 1000 wt. ppm), tend to fracture at room temperature before reaching 0.5-1.0% plastic strain in tension. Engineering alloys based on the  $\gamma$ -TiAl phase usually have Al concentrations of 45-48 at.% and thus solidify peritectically according to the phase diagram shown in Figure 1 [1,7]. After solidification, binary  $\gamma$ -TiAl alloys pass through the single-phase field of  $\alpha$  solid solution, which decomposes on further cooling according to the reactions  $\alpha \to \alpha + \gamma \to \alpha_2 + \gamma$  or  $\alpha \to \alpha_2 \to \alpha_2 + \gamma$ .

The mechanical behavior of TiAl alloys strongly depends on their composition and in particular there is a considerable difference between single-phase and two-phase alloys [8,9]. The two-phase TiAl with Ti-rich compositions (Ti-48 at.% Al) shows higher strength and better ductility than the single-phase TiAl. The Al-rich single-phase TiAl has few deformation twins at room temperature. At elevated temperatures, where the ductility is rapidly improved with decreasing strength, the formation of twins and extended faults on the {111} plane becomes more frequent. Twinning deformation becomes dominant in Ti-rich two-phase alloys, even at room temperature. Such different twinning activity in Ti-rich and Al-rich alloys is one of the reasons why the former alloys are more ductile than the latter.

Although a lot of progress has been made in the research and development of  $\gamma$ -TiAl-based alloys, the low room-temperature ductility restricts the use of these materials as a new class of engineering materials. It is well known that the microstructure and mechanical properties of TiAl alloys are strongly influenced by the alloy composition. The presence of 3 at.% Cr in Ti-45Al-3Cr (at.%) produces B2 phase and thus improves the tensile ductility, but lowers the yield strength [10]. The former effect may be attributed to the more uniform plastic deformation in the Cr-modified lamellar microstructure, while the latter could be caused by the thickening of the  $\gamma$  lamellae. In another study, B2 phase was introduced to the TiAl alloy by adding 2 at.% Mo to Ti-44Al-2Mo (at.%), hence

improving room-temperature tensile ductility and strength [11]. However, according to the study carried out by Sun, *et al.* [11], presence of B2 phase in TiAl alloys does not improve strength and ductility at room temperature, but decreases them [12]. Moreover, the appearance of B2 phase also deteriorates creep resistance and high-temperature strength.

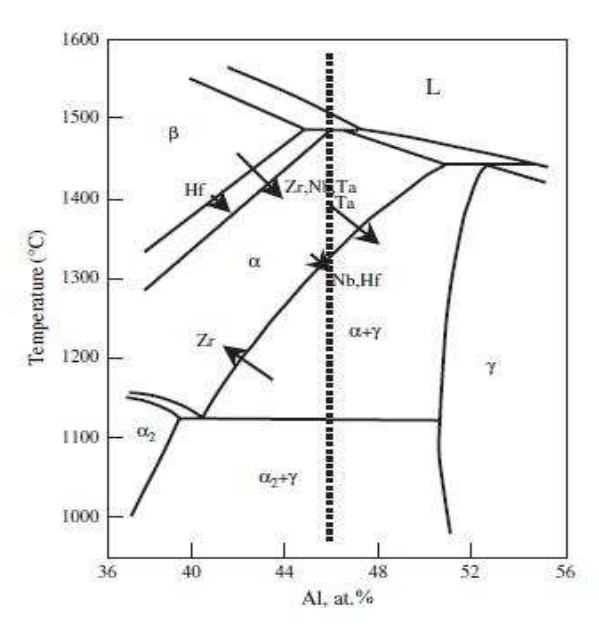


**Figure 1** A typical section of Binary Ti-Al Phase diagram with the arrows demonstrating the movement of the phase boundaries for ternary alloying additions and their length representing the strength of each element [7].

The presence of Cr and Mn in TiAl alloys could enhance their ductility. This is caused by the ability of these elements to stabilize thermal twins, which are nucleation sites for twinning dislocations, and also to decrease the Ti 3p and Al 3p binding energies in Ti-Ti, Ti-Al, and Al-Al bonds [13,14]. If a small amount of W (up to 0.4 at.%) is added to TiAl-Nb-W-B alloys, their grain sizes will refine and the lamellar spacing will be reduced as well [15]. Grain size refinement and solution strengthening through W addition contribute to an increased hardness of TiAl alloys. Alloying elements, such as Mo and Nb, can improve tensile strength at room and elevated temperatures, but have little effect on improving room-temperature ductility [9,16]. The strength of TiAl alloys can also be enhanced by adding Ru (up to 1.4 at.%). For the heat-treated samples, TiAl-Ru exhibits a better strengthening effect than TiAl-Nb [17]. In room-temperature flexural tests, the ductility of TiAl-Ru is also better than that

of TiAl-Nb. TiAl-Ru indicates much larger flexural strain and fracture energy than TiAl-Nb.

Only a very limited number of studies associated with the effect of a combined addition of Cr and Mo on room-temperature fracture strain and strength has been conducted. This study was aimed at resolving some of the lack of information about this subject. It will be reported that the addition of both Cr and Mo to the as-cast Ti-48Al alloy produced in a locally made arc-melting furnace showed better mechanical properties in terms of yield strength and fracture strain in compression.

# 2 Experimental Set-up

The raw materials used in this study were powders of titanium (average size of 83.81 µm and purity of 99.7%, STREM Chemicals), aluminum (average size of 72.53 µm and purity of 95.7%, BDH Laboratory supplies), molybdenum (average size of 122 µm and purity of 99.96%, STREM Chemicals), and chromium (average size of 50.92 µm and purity of 99%, STREM Chemicals). The powders were weighted to the desired compositions of Ti-48Al, Ti-48Al-2Cr and Ti-48Al-2Cr-2Mo (all in at.%). The compositions were thoroughly mixed in a plastic PE bottle for 5 hours. The mixture was then compacted in a die by applying a hydraulic press with a pressure of 100 MPa. The size of pellet was 25 mm in diameter. The pellets were then melted using a locally made arcmelting furnace as shown in Figure 2 [18,19]. The ingots were re-melted eight times to ensure good homogeneity. The resulting samples will be referred to as as-cast TiAl alloys.

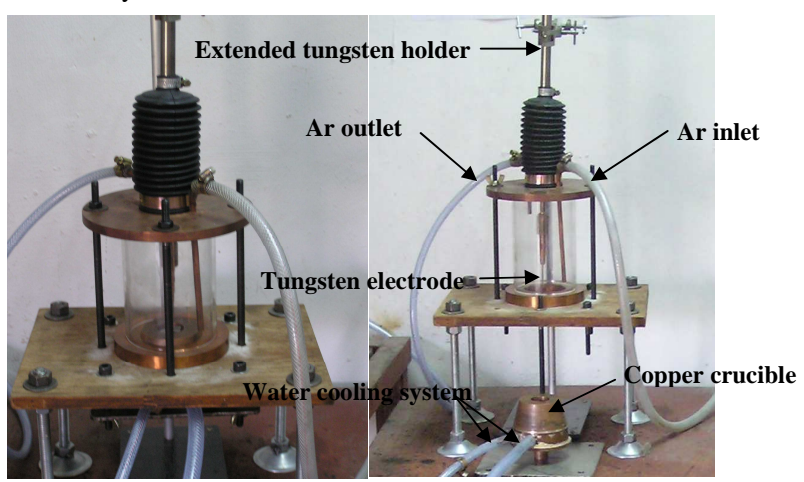


Figure 2 Photograph of locally made arc-melting furnace.

A diamond-coated blade cutting tool was used to cut the as-cast TiAl alloys into metallographic and compressive samples. The metallographic samples were polished and then etched in a solution of 10 vol.% HNO<sub>3</sub>, 5 vol.% HF, and 85 vol.% water [20]. X-ray diffraction (XRD) using a diffractometer (Siemens D5000) with Cu K $\alpha$  anode ( $\lambda$  = 1.54056 Å) was used to identify the phases present in the samples. A SEM back-scattered scanning electron microscope (model SUPRA 35VP) combined with energy dispersive spectroscopy (EDS) was used to predict the phases formed and to observe the microstructure. SEM micrographs were also used to analyze the fracture surfaces of the compressed alloys.

A Rockwell hardness test was performed in accordance with ASTM standard E 18-98 [21] using a Rockwell type hardness tester (LECO). A Rockwell C scale with a load of 150 kg that employed a diamond point (Brale indenter) was used. In this study, the samples produced were small in size and therefore tensile tests could not be performed. However, compression tests have many similarities to tension tests in the manner of conducting the test and the analysis, as well as in the interpretation of the results [22-24]. TiAl samples with a small size can be employed appropriately in compression tests. Specimens measuring 7 X 7 X 14 mm were cut and used for the compression tests. All specimens were polished before testing. The compression tests were carried out at room temperature with an Instron servohydraulic testing machine with a crosshead speed of 0.07 mm/min, in accordance with ASTM E9-89a [25]. Also, a secondary scanning electron microscope was used to observe the fracture surfaces of the samples.

#### 3 Results and Discussion

#### 3.1 X-Ray Diffraction Patterns

Figure 3 shows the XRD patterns of the as-cast TiAl alloys produced by arcmelting. It can be seen from the diffraction results that Ti-48Al predominantly contains  $\gamma$  phase and a minor amount of  $\alpha_2$  phase (Figure 3(a)). This was expected, as discussed previously, since the equilibrium Ti-Al binary phase diagram (see Figure 1) indicates the presence of two phases for the nominal composition of Ti-48Al. Similarly,  $\gamma$ -TiAl as the main phase and  $\alpha_2$ -Ti<sub>3</sub>Al as the secondary phase were also identified in the other two as-cast alloys with the addition of alloying elements Cr and Mo (Figure 3(b) and 3(c)).

Figure 3(b) shows that with the addition of 2 at.% Cr, the XRD profile of Ti-48Al-2Cr exhibited a significant decrease in intensity of the first and strongest peak, which belongs to the  $\gamma$  phase. This indicates that the addition of Cr had an effect on the XRD profile of the Ti-48Al alloy. On the other hand, a combined

addition of Cr and Mo to Ti-48Al indicated a very slight decrease in intensity of the first and strongest peak, belonging to the  $\gamma$  phase (Figure 3(c)). This result was expected, as the addition of alloying elements up to 4 at.% does not significantly change the constitution of TiAl alloys in which  $\gamma$  is the major phase and  $\alpha_2$  is the minor phase and no brittle and hard phase, for example B2 phase, was identified [1,12].

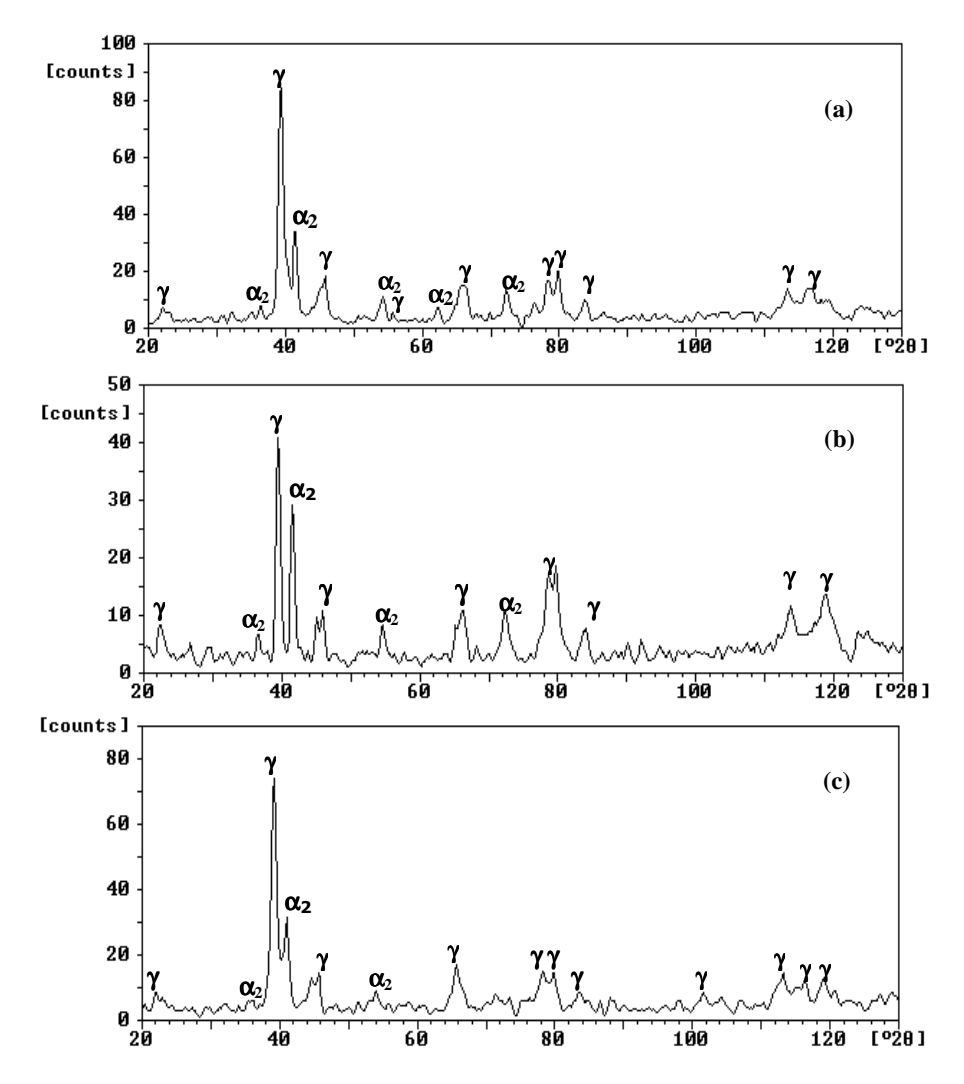


**Figure 3** XRD patterns of as-cast alloys (a) Ti-48Al, (b) Ti-48Al-2Cr, and (c) Ti-48Al-2Cr-2Mo.

# 3.2 Microstructure of As-Cast TiAl Alloys

Figure 4 shows the back-scattered scanning electron micrographs that represent the microstructures of the as-cast TiAl samples produced by arc-melting. Based on the EDS analysis (Table 1), primary  $\gamma$  phase was identified, as well as lamellar colonies consisting of alternate  $\alpha_2$  and  $\gamma$  phases. The microstructure of the as-cast Ti-48Al exhibited a duplex microstructure, consisting of a small amount of primary  $\gamma$  phase, and  $(\alpha_2 + \gamma)$  lamellar colonies (Figure 4(a)).

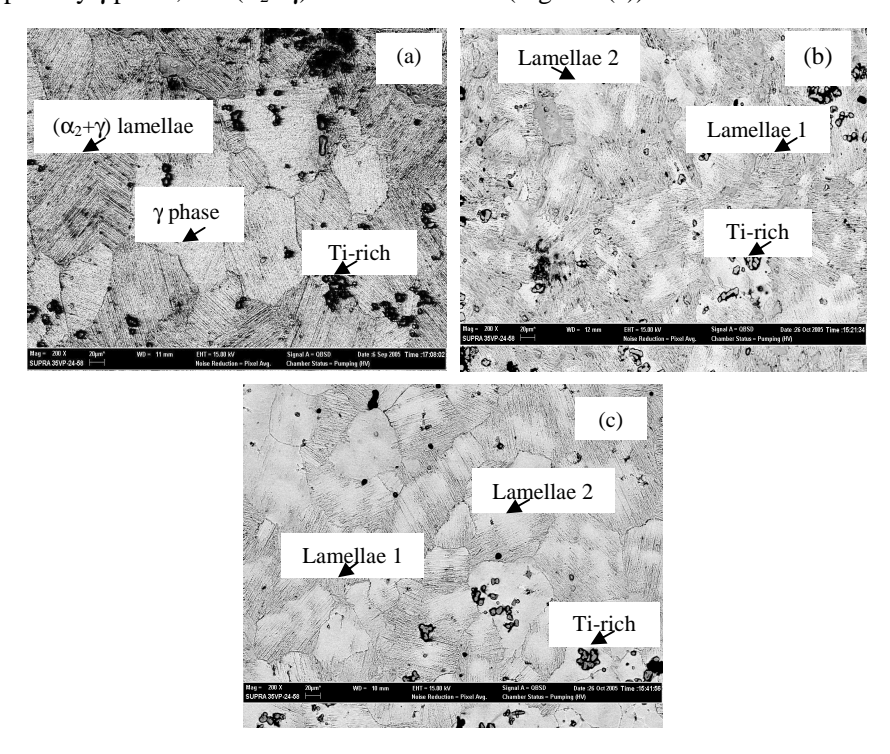


**Figure 4** The back-scattered SEM micrographs showing the microstructures of the as-cast TiAl alloys: (a) Ti-48Al, (b) Ti-48Al-2Cr and (c) Ti-48Al-2Cr-2Mo. Note (a): duplex microstructure, (b) and (c): nearly lamellar microstructure.

With the presence of Cr in Ti-48Al-2Cr, it can be said that the microstructure reveals a nearly lamellar microstructure consisting of alternate  $\alpha_2$  and  $\gamma$  phases (Figure 4(b)). On the basis of the EDS analysis, the lamellar regions marked as lamellae 2 are believed to be lamellar phases as well. In this study, even though a strong etching solution has been applied, as mentioned in the experimental set-up section, it was hard to reveal complete lamellar structures in the lamellae-2 regions. The addition of Cr and Mo to Ti-48Al also resulted in a nearly

lamellar microstructure comprising of alternate  $\alpha_2$  and  $\gamma$  phases (Figure 4(c)). It was found that complete lamellar structures could not be revealed in regions marked as lamellae 2 in the microstructure of Ti-48Al-2Cr-2Mo.

TiAl alloys	Phases	Ti (at.%)	Al (at.%)	Cr (at.%)	Mo (at.%)	C (at.%)
Ti-48Al	γ	45.98	54.02	-	-	-
	$(\alpha_2+\gamma)$	54.63	45.37	-	-	-
	Ti-rich	68.01	-	-	-	31.99
Ti-48Al-2Cr	$(\alpha_2+\gamma)$ 1	49.86	48.23	1.91		
	$(\alpha_2+\gamma)$ 2	50.23	48.08	1.69	-	-
	Ti-rich	69.97		-		30.03
Ti-48Al-2Cr-2Mo	$(\alpha_2+\gamma)$ 1	48.91	45.74	2.91	2.44	-
	$(\alpha_2+\gamma)$ 2	51.61	44.85	1.4	2.13	-
	Ti-rich	69.5	-	-	-	30.85

**Table 1** Results of EDS analysis for as-cast TiAl alloys.

In addition, it can also be observed that the lamellar colonies were randomly oriented in all the samples. Some Ti-rich precipitates in the phases and at grain boundaries were also apparent, which consisted of 68.01 at.% Ti and 31.99 at.% C based on the EDS analysis (Table 1). It is suspected that the carbon most likely came from the tungsten-carbide electrode used [26]. This element has a strong tendency to react with Ti at melting temperature [1,27].

#### 3.3 Hardness of TiAl Alloys

The average hardness results of the as-cast TiAl alloys are shown in Figure 5. It can be seen that the hardness of the as-cast TiAl alloys are relatively high, exceeding 50 HRC. The hardness values of the different alloys exhibited little variation. With the addition of alloying elements Cr, Mo, or a combination of both, the hardness values increased slightly as compared to the Ti-48Al alloy. In this case, the hardness of the TiAl alloys showed a weak sensitivity to the presence of a small amount of the alloying elements.

# 3.4 Effect of Cr and Mo on Compressive Yield Strength and Fracture Strain

The yield strength results obtained from the compression tests for the as-cast TiAl alloys are shown in Figure 6. It can be seen that the presence of Mo in Ti-48Al-2Cr-2Mo alloy resulted in an increase in yield strength. The as-cast TiAl alloys show the dependence of yield strength on the presence of Mo. Solid solution strengthening due to the addition of Mo most likely contributed to the increased yield strength of Ti-48Al-2Cr-2Mo. Even though the presence of Cr in the Ti-48Al-2Cr alloy showed a slightly increased yield strength in compression, its

effect was insignificant in this case, and it is believed that it did not play a role in the solid solution strengthening of the alloys.

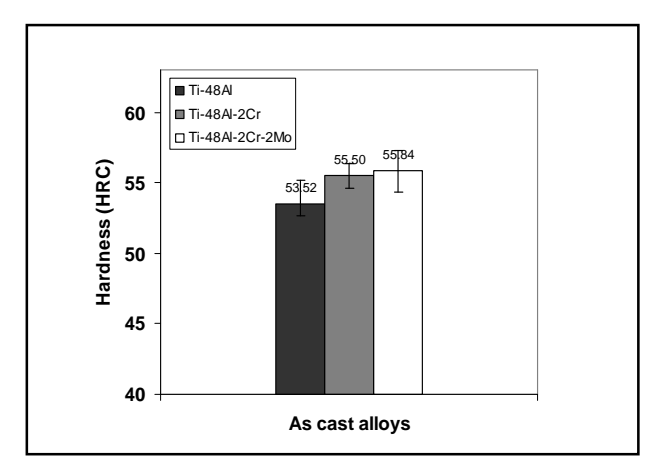
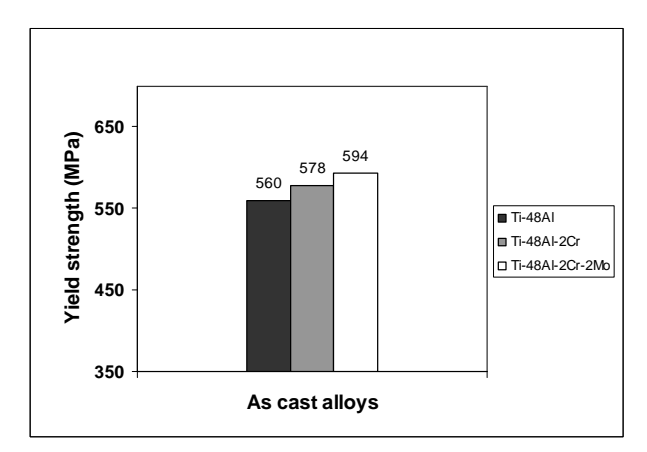
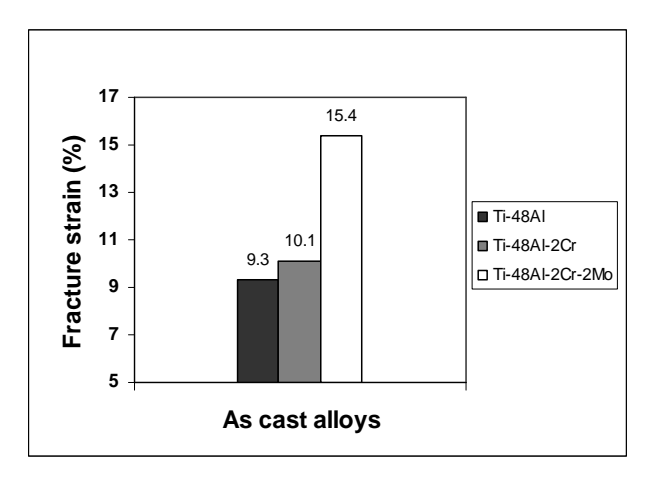


Figure 5 Rockwell hardness values of Ti-48Al, Ti-48Al-2Cr, and Ti-48Al-2Cr-2Mo



**Figure 6** Compressive yield strength of Ti-48Al, Ti-48Al-2Cr and Ti-48Al-2Cr-2Mo alloys.

Strain to fracture in compression of the different as-cast TiAl alloys is shown in Figure 7. With the addition of Cr, the fracture strain of as-cast Ti-48Al-2Cr slightly increased, to 10.1. The presence of Cr in Ti-48Al-2Cr-2Mo gave the highest fracture strain (up to 15.4%). Therefore, it can be said that the as-cast Ti-48Al-2Cr-2Mo alloy exhibited a higher yield strength and fracture strain in compression as compared to the other as-cast TiAl alloys.



**Figure 7** Compressive fracture strain of as-cast Ti-48Al, Ti-48Al-2Cr, and Ti-48Al-2Cr-2Mo.

#### 3.5 Fracture Behavior

Figure 8 shows SEM micrographs of the fracture surfaces of the as-cast TiAl alloys after the compression test at room temperature. The fracture surfaces of the as-cast TiAl alloys were mixed transgranular and interlamellar fracture modes in which cleavage facets were dominant. Due to the layered structure of the lamellae, a step-like transgranular fracture of the lamellae was also apparent, particularly in the fracture surfaces of Ti-48Al-2Cr-2Mo (see the enlarged micrograph of Figure 8(c)). The typical cleavage facets observed were without the appearance of flat and featureless facets.

#### 4 Conclusions

Ti-48Al exhibited a duplex microstructure. The presence of 2 at.% Cr in Ti-48Al-2Cr and the presence of both Cr and Mo in Ti-48Al-2Cr-2Mo produced a nearly lamellar microstructure. The hardness values increased slightly as compared to the Ti-48Al alloy after addition of Cr and Mo. It was found that the fracture strain of the as-cast TiAl alloy slightly increased with the addition of Cr. In this study, the as-cast Ti-48Al-2Cr-2Mo alloy exhibited a better strength and fracture strain as compared to the other as-cast TiAl alloys. The mixed brittle transgranular and interlamellar fracture modes were predominantly observed on the fracture surfaces of the as-cast TiAl alloys.

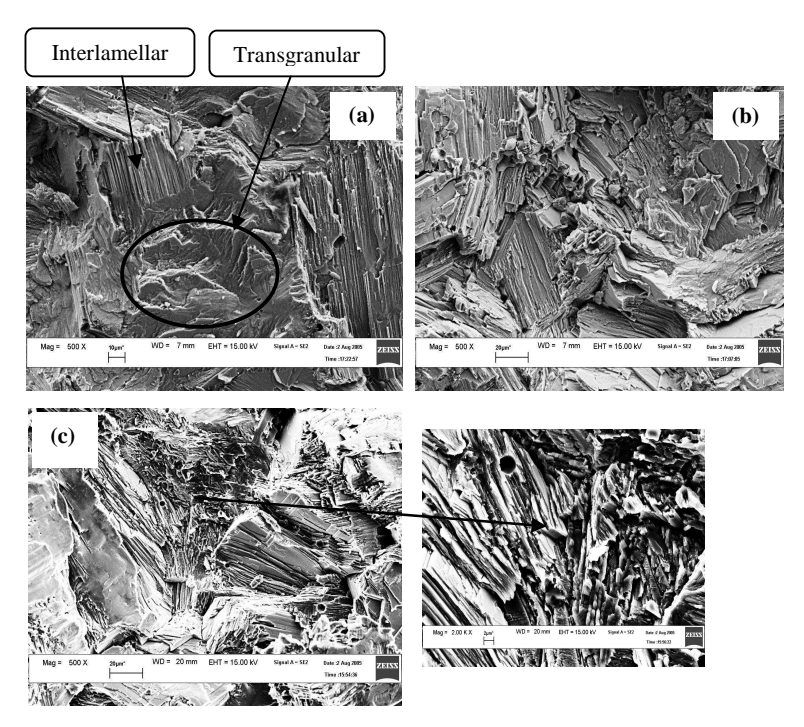


**Figure 8** SEM micrographs showing fracture surfaces of as-cast TiAl alloys (a) Ti-48Al, (b) Ti-48Al-2Cr, and (c) Ti-48Al-2Cr-2Mo alloys after compression testing.

### Acknowledgements

The authors would like to acknowledge AUN/SEED-net/JICA for providing the research fund. We are also grateful to Dr. Sunara Purwadaria, Department of Metallurgical Engineering, FTTM, ITB, for his great assistance and suggestions for the engineering design and building of the locally made arc-melting furnace.

#### References

- [1] Appel, F. & Oehring, M., *y-Titanium Aluminide Alloys: Alloy Design and Properties*, Titanium and Titanium Alloys, Leyens, C. & Peters, M. (eds.), Weinheim: Wiley-VCH, pp. 89-152, 2003.
- [2] Wilshire, W., Recent Developments in Materials for High Temperature Service, International Conference on Recent Advances in Materials and Minerals, Universiti Sains Malaysia, Pulau Penang, 24-26 June, pp. 1-10, 1994.

- [3] Dimiduk, D.M., Gamma Titanium Aluminide Alloys-An Assessment within the Competition of Aerospace Structural Materials, Mater. Sci. and Eng. A, 263(2), pp. 281-288, 1999.
- [4] Yamaguchi, M., Inui, H. & Ito, K., *High-Temperature Structural Intermetallics*, Acta Materialia, **48**(1), pp. 307-322, 2000.
- [5] Voice, W., *Practical Advice on the Use of Ti-45-2-2-XD*<sup>TM</sup> *Gamma Titanium Aluminide*, Titanium Alloys at Elevated Temperature: Structural Development and Service Behavior, Winstone, M.R. (ed.), London: IOM Communications Ltd., pp. 237-250, 2001.
- [6] Kim, Y.M., *Strength and Ductility in TiAl Alloys*, Intermetallics, **6**(7), pp. 623-628, 1998.
- [7] Wu, X., Review of Alloy and Process Development of TiAl Alloys, Intermetallics, 14, pp. 1114-1122, 2006.
- [8] Umakoshi, Y., *Intermetallics*, Volume 8: Structure and Properties of Nonferrous Alloys, Cahn, C.W., Haasen, P. & Kramer, E.J. (eds.), Weinheim: Wiley-VCH. pp.263-291, 1996.
- [9] Marketz, W.T., Fischer, F.D. & Clemens, H., *Deformation Mechanisms in TiAl Internetallics-Experiments and Modeling*, Inter. J. of Plasticity, **19**, pp. 281-321, 2003.
- [10] Zheng, Y., Zhao, L., & Tangri, K., Effect of Cr Addition and Heat Treatment on the Microstructure and Tensile Properties of A Cast Ti-45Al-3Cr (at.%) alloy, Mater. Sci. and Eng. A, 208, pp. 80-87, 1996.
- [11] Li, Y.G. & Loretto, M.H., *Microstructure and Fracture Behavior of Ti-44Al-xM derivatives*, Acta Metall. Mater., **42**(9), pp. 2913-2920, 1994.
- [12] Sun, F.-S., Cao, C.-X., Kim, S.-E., Lee, Y.-T. & Yan, M.-G., *Alloying Mechanism of Beta Stabilizers in a TiAl Alloy*, Metallurgical & Materials Transaction, **32A**(7), pp. 1573-1589, 2001.
- [13] Jin, Y., Wang, J.N., Wang, Y., & Yang, J., Effect of Mn on Formation of Lamellar Structure in a TiAl Alloy, Materials Letters, **58**(29), pp. 3756-3760, 2004.
- [14] Wang, Y., Wang, J.N., Yang, J., & Zhang, B., Control of a Fine-Grained Microstructure for Cast High-Cr TiAl Alloys, Mate. Sci. and Eng. A, 392 (1-2), pp. 235-239, 2005.
- [15] Huang, L., Liaw, P.K., & Liu C.T., *Microstructural Control of Ti-Al-Nb-W-B alloys*, Metallurgical & Materials Transactions A, **38**(13), pp. 2290-2297, 2007.
- [16] Krumla, T., Petreneca, M., Obrtlika, K., Polaka, J. & Bucek, P., *Influence of Niobium Alloying on The Low Cycle Fatigue of Cast TiAl Alloys at Room and High Temperatures*, Procedia Engineering, **2**(1), pp. 2297-2305, 2010.
- [17] Liu, Q. & Nash, P., The Effect of Ruthenium Additions on The Microstructure and Mechanical Properties of TiAl Alloys, Intermetallics, 19, pp. 1282-1290, 2011.

- [18] Kestler, H. & Clemens, H., *Production, Processing and Application of* γ(*TiAl*)-Based Alloys, Titanium and Titanium Alloys, Leyens, C. & Peters, M., eds., Weinheim: Wiley-VCH, pp. 351-392, 2003.
- [19] Usman, H., Mohd. Noor, A.F & Astrawinata, R., Mechanical Properties and Microstructure of TiAl Alloys Produced by Locally Made Arc-Melting Process, International Conference on Recent Advances in Mechanical and Materials Engineering, University of Malaya, Kuala Lumpur, 30-31 May, pp. 1313-1317, 2005.
- [20] Chen, J.H., Cao, R., Wang, G.Z. & Zhang, J., Study on Notch Fracture of TiAl Alloys at Room Temperature, Metallurgical & Materials Transaction, 35A (2), pp. 439-456, 2004.
- [21] ASTM E18-98, Standard Test Methods for Rockwell Hardness and Rockwell Superficial Hardness of Metallic Materials, American Standard for Testing Materials, **03.01**, pp. 116-129, 1999.
- [22] Dowling, N.E., *Mechanical Behavior of Materials*, 2<sup>nd</sup> ed., New Jersey: Prentice-Hall Inc, pp. 210-218, 1999.
- [23] Meyers, M.A. & Chawla, K.K., *Mechanical Behavior of Materials*, pp. 300-305, 1<sup>st</sup> ed., New Jersey: Prentice-Hall Inc., 1999.
- [24] Calderon, H.A., Garibay-Febes, V., Umemoto, M., & Yamaguchi, M., *Mechanical Properties of Nanocrystalline Ti-Al-X alloys*, Mater. Sci. and Eng. A, **329-331**, pp. 196-205, 2002.
- [25] ASTM E9-89a, Standard Test Methods for Compression Testing of Metallic Materials at Room Temperature, American Standard for Testing Materials, **03.01**, pp. 99-106, 1999.
- [26] Usman, H., Mohd. Noor, A.F. & Astrawinata, R., *Microstructure and Fracture Observation of Hot-Pressed and as-Cast TiAl-Based Alloys*, Malaysian Journal of Microscopy, **2**, pp. 196-205, 2006.
- [27] Rosenqvist, T., *Principles of Extractive Metallurgy*, 2<sup>nd</sup> ed., Trondheim: Tapir Academic Press, pp. 492, 2004.